

## Resistance of a Single Domain Wall in (Co/Pt)<sub>7</sub> Multilayer Nanowires

C. Hassel,<sup>1,\*</sup> M. Brands,<sup>1</sup> F. Y. Lo,<sup>2</sup> A. D. Wieck,<sup>2</sup> and G. Dumpich<sup>1</sup>

<sup>1</sup>*Fachbereich Physik, Experimentalphysik, Universität Duisburg-Essen, 47048 Duisburg, Germany*

<sup>2</sup>*Lehrstuhl für Angewandte Festkörperphysik, Ruhr-Universität Bochum, 44780 Bochum, Germany*

(Received 12 June 2006; published 30 November 2006)

Single (Co/Pt)<sub>7</sub> multilayer nanowires prepared by electron beam lithography with perpendicular magnetic anisotropy are locally modified by means of Ga-ion implantation generating 180° domain walls which are pinned at the edges of underlying thin Pt wires. Since we can exclude contributions from the anisotropic and the Lorentz magnetoresistance this allows us to determine the resistance of a single domain wall at room temperature. We find a positive relative resistance increase of  $\Delta R/R = 1.8\%$  inside the domain wall which agrees well with the model of Levy and Zhang [Phys. Rev. Lett. **79**, 5110 (1997)].

DOI: [10.1103/PhysRevLett.97.226805](https://doi.org/10.1103/PhysRevLett.97.226805)

PACS numbers: 73.21.Ac, 75.60.Ch, 75.75.+a

Since the first observation of the domain wall resistance (DWR) in iron whiskers [1], it has become a topic of great interest to understand the principles of the DWR, experimentally as well as theoretically. However, the experimental as well as theoretical results are controversial. Whereas the model of Levy and Zhang predicts a positive DWR due to the spin mistracking inside the domain wall [2], the model of Tataru and Fukuyama predicts a negative DWR due to the dephasing of the electron waves inside the domain wall originating from reduced weak electron localization (WEL) [3]. Van Gorkom, Brataas, and Bauer found that the DWR can be either positive or negative depending on spin-dependent scattering times [4]. Many experiments on metallic wires show either a positive [5,6] or a negative contribution [7]. For a recent review, see [8]. To determine the DWR, it is important to exclude all other magnetoresistance (MR) contributions like the Lorentz MR (LMR) [9] or the anisotropic MR (AMR) [10].

Most of the recent experiments have been carried out using magnetic thin films or nanowires with in-plane magnetic anisotropy. However, even if LMR and AMR contributions are carefully subtracted, the spin configuration inside the Néel wall itself contributes to the AMR. Thus, most promising candidates for investigating the DWR are magnetic systems with out-of-plane anisotropy where magnetic domains are separated by Bloch walls [6]. Recently, we have shown that (Co/Pt)<sub>n</sub> multilayer (ML) nanowires with out-of-plane anisotropy are a suitable system and exhibit a positive DWR at low temperatures [11]. However, these experiments did not allow us to determine the DWR quantitatively, since we could not determine the exact number of domain walls.

In this Letter we report on MR measurements at room temperature where we achieved the nucleation and the pinning of a single domain wall in a polycrystalline (Co/Pt)<sub>7</sub> ML-nanowire controlled by magnetic force microscopy (MFM) measurements. This allows us to determine the DWR directly, i.e., contributions from AMR and LMR can be neglected.

Single (Co/Pt)<sub>7</sub> ML nanowires are prepared by high resolution electron beam lithography (HR-EBL) with lift-off technique. We use a special resist system which enables us to fabricate wires with no tear-off edges down to widths of about 100 nm [12]. Co and Pt are electron beam evaporated from independent crucibles at a base pressure of  $7 \times 10^{-9}$  mbar [13]. The (Co/Pt)<sub>7</sub> ML nanowires are grown at room temperature on a Pt buffer layer with a thickness of  $t = 5$  nm. The layer sequence is 7 times 2.5 Å Co and 9.5 Å Pt, respectively, followed by a 1 nm thick Pt cap layer to prevent oxidation of Co.

MR measurements using an ac-resistance bridge operating with low currents of  $I \approx 1 \mu\text{A}$  allow us to determine the resistance with a resolution better than  $10^{-5}$ . Magnetic fields up to 2 T are applied at room temperature using an electromagnet. Detailed analyses of the domain patterns and the magnetization reversal mechanisms are carried out via MFM at room temperature. It is possible to apply magnetic fields up to 100 mT perpendicular to the sample plane during imaging.

Figure 1 shows a secondary electron micrograph (SEM) image of a (Co/Pt)<sub>7</sub> ML nanowire with a width of  $w = 130$  nm. In this high resolution image the polycrystalline structure of the wire is visible. Note that the wire has nearly no edge roughness and no tear-off edges. With transmis-

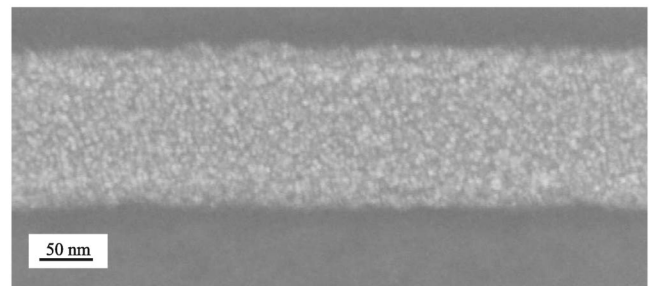


FIG. 1. SEM image of a (Co/Pt)<sub>7</sub> ML wire with a width of 130 nm. The polycrystalline structure of the wire is visible. No tear-off edges are present showing the high quality of the fabrication procedure.

sion electron microscopy investigations, we determined a mean grain size of  $(6 \pm 2)$  nm. From electron diffraction we find that the crystal structure is fcc, whereby Co adopts the crystal structure of Pt.

Figure 2 shows the Kerr-rotation angle  $\Phi$  of a  $(\text{Co/Pt})_7$  ML film versus magnetic field applied perpendicular to the film plane. The remanent state is single domain which reverses at a coercive field of  $\mu_0 H_C = 20$  mT into the opposite single domain state. SQUID measurements confirm this magnetization reversal behavior and a saturation magnetization of  $M_S = 1080$  kA m $^{-1}$  is determined [14]. From in-plane MR measurements on  $(\text{Co/Pt})_7$  ML nanowires we obtain an effective magnetic anisotropy constant of  $K_{\text{eff}} = 1.05 \times 10^6$  J m $^{-3}$  using the procedure described in Ref. [15]. We find  $Q$  values [ $Q = K_{\text{eff}}/(\frac{1}{2}\mu_0 M_S^2)$ ] of about  $Q = 1.5$  which indicates that flux closure domains should not be present [16].

To nucleate a domain wall on a distinct site of the wire, we used Ga-ions which are implanted locally by means of a focused ion beam. It is known that Ga-ion implantation with low doses reduces the coercive field of  $(\text{Co/Pt})_7$  ML films [17,18]. Figure 3 displays the results of the MFM investigations [Fig. 3(b)–3(f)] as well as an atomic force microscopy (AFM) image of the structure [Fig. 3(a)]. The dashed lines indicate the positions where Ga-ions with a dose of the order of  $I \approx 10^{13}$  ions cm $^{-2}$  were implanted. The width of the implanted area is less than 100 nm given by the beam diameter. No structural changes of the  $(\text{Co/Pt})_7$  ML wire are observable in the AFM image. MFM images are taken after presaturation of the  $(\text{Co/Pt})_7$  ML wire as well as the tip in a magnetic field of  $-100$  mT, which is well above the coercive fields of single wires ( $\mu_0 H_C \approx 30$  mT) and the tip ( $\mu_0 H_C \approx 50$  mT). The first MFM image [Fig. 3(b)] was taken in remanence and shows that the wire is in a single domain state. By applying small magnetic fields [Fig. 3(c)] well below the coercive field of unmodified wires, reversed domains begin to grow at the positions of the Ga-ion implantation. By increasing the magnetic field, the reversed domains expand [Fig. 3(d)]. The domain walls

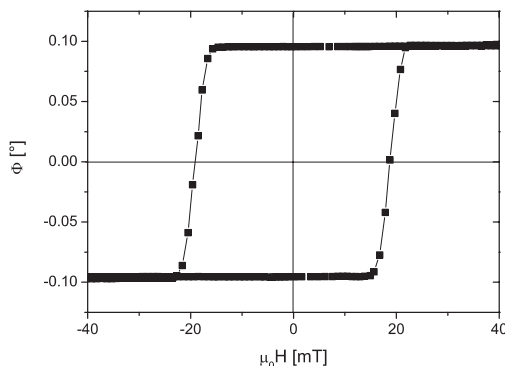


FIG. 2. Dependence of the polar Kerr angle of a  $(\text{Co/Pt})_7$  ML film versus the external magnetic field perpendicular to the film plane.

move through the wire and are stopped due to intrinsic pinning sites [Fig. 3(e)]. The pinning is weak since the domain walls move further when the external magnetic field is slightly increased [Fig. 3(f)]. The magnetization of the wire is completely reversed at 22.6 mT which is smaller as compared to an unmodified wire.

The fact that the domain walls move easily through the wire requires us to pin the domain walls. Therefore, we prepare single  $(\text{Co/Pt})_7$  ML nanowires on top of thin Pt wires ( $t = 5$  nm) in a multistep EBL process [12]. MFM investigations on such structures are presented in Fig. 4. Figure 4(a) is an AFM image and shows the structure of the sample. The  $(\text{Co/Pt})_7$  ML nanowire (from bottom to top) is placed perpendicular on top of two platinum wires (horizontal). A dashed line indicates the position, where Ga-ions with a dose of  $I \approx 10^{13}$  ions cm $^{-2}$  were implanted. In remanence [Fig. 4(b)], the wire is in a single domain state. By applying a magnetic field, a reversed domain is nucleated in the implanted area, whereby two domain walls are created which start to propagate. Because of the vertical modification of the  $(\text{Co/Pt})_7$  ML wire by the Pt, the domain wall propagation is suppressed and the two domain walls are pinned at the edges of the underlying Pt wires [Fig. 4(c)]. In a magnetic field range of about  $\mu_0 \Delta H = 8$  mT the two domain walls are stable [Fig. 4(d)]. By further increasing the magnetic field, the domain walls are depinned [Fig. 4(e)], and the whole wire is reversed [Fig. 4(f)]. Note that the MFM contrast at the implantation position is slightly lower than in the other parts of the wire. This is due to the reduced Curie temperature and, thus, the reduced magnetization at room temperature of the implanted part of the wire [19]. We have characterized each wire used for the MR measurements separately by MFM. They all show the same reversal behavior as shown in Fig. 4.

In a third EBL step, the structures are contacted with *nonmagnetic* Au contact pads close to the implanted area which serve as contacts to measure the four point resistance. Figure 5 shows a SEM image of the structure used for the DWR measurements where the center area is magnified. It has been shown by MFM investigations that the Au

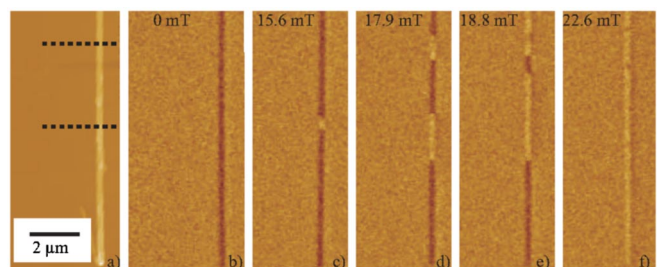


FIG. 3 (color online). AFM image of the investigated structure (a). The wire has a width of 312 nm. The dashed lines indicate the ion implantation position. The MFM images were taken after presaturation in a magnetic field of  $-100$  mT perpendicular to the film plane. Reversed domains are nucleated at the implantation positions.

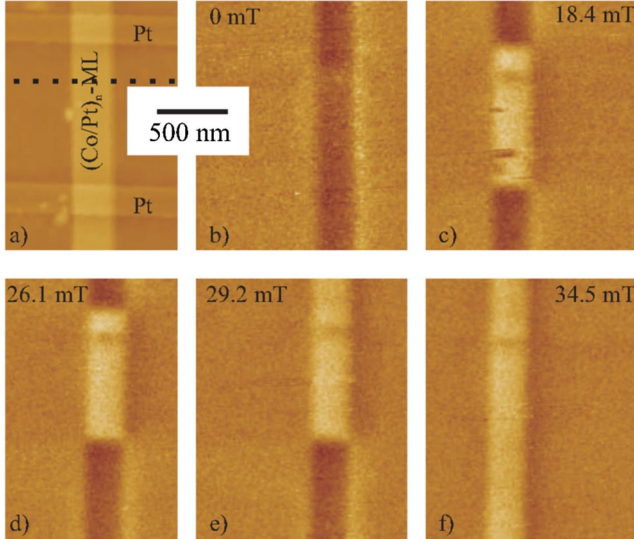


FIG. 4 (color online). AFM image of the investigated structure (a). The dashed line indicates the ion implantation position. Note that the Pt wire is below the  $(\text{Co/Pt})_7$  ML wire with a width of 450 nm. The MFM images were taken after saturation in a magnetic field of  $-100$  mT. Single domain walls are pinned at the edges of the Pt wires.

contacting has no influence on the magnetization reversal process [14]. Since the Pt wires serve as pinning centers for the domain walls using only one Pt wire instead of two allows to pin a single domain wall.

Figure 6 shows a MR measurement at room temperature of a similar structure as shown in Fig. 5 with only one Pt wire as pinning center. The MFM images taken in the vicinity of the Ga-ion implanted region at the saturation field, in remanence, and when one domain wall is pinned illustrate the respective domain configuration of the  $(\text{Co/Pt})_7$  ML nanowire. Note, that the MFM contrast is the same in positive and negative fields since the magnetization of the tip reverses as well. The MR taken at room temperature reveals a hysteretic behavior as indicated by the arrows. The measurement is symmetric with respect to the magnetic field direction, and shows a resistance decrease for higher magnetic fields, which is known as the spin-disorder MR [20]. Starting from saturation the resistance increases continuously and behaves reversible as long as the field direction is not reversed (red circles). The resistance maxima only occur when the magnetization reversal process induces a domain wall as indicated by the insets. This unambiguously shows that the presence of a single domain wall gives rise to a positive resistance contribution. Because of the depinning of the single domain wall, one would expect a sharp resistance decrease. In contrast, the resistance data in Fig. 6 show a continuous decrease spread over several data points. Our measurements are carried out at room temperature which leads to temperature fluctuations of the order of  $\Delta T \approx 10$  mK. According to a temperature coefficient of the resistance of  $\alpha \approx 6 \times 10^{-4}$  this causes a resistance variation of

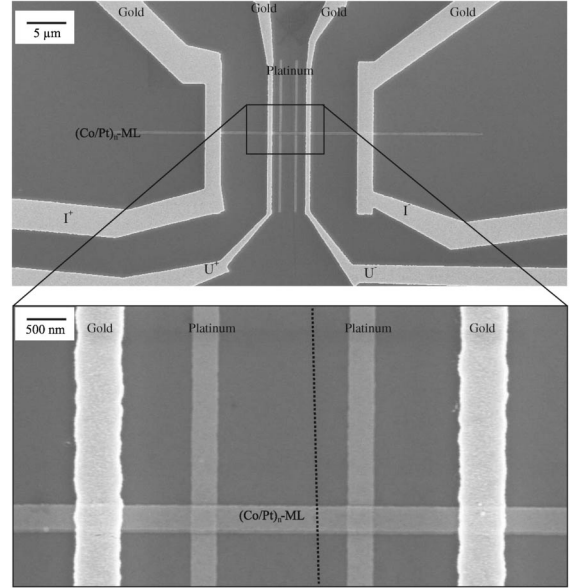


FIG. 5. SEM image of a  $(\text{Co/Pt})_7$  ML wire with a width of 313 nm on top of two underlying Pt wires. Between the two Pt wires Ga-ions with a dose of  $1 \times 10^{13}$  ions/cm<sup>2</sup> were implanted. The position is sketched by the dashed line. The Au contacts are in the vicinity of the domain walls allowing to determine the resistance change with high resolution.

$\delta R/R$  of about  $1 \times 10^{-5}$ , which is about one third of the observed resistance increase  $\Delta R/R$  in Fig. 6. To improve the signal to noise ratio, our data are averaged over four measurement cycles. We have found that this procedure results in smaller resistance fluctuations rather than measuring at fixed magnetic fields.

In our experiment, the resistance is measured between the voltage leads with a distance of  $L = 2.6 \mu\text{m}$ , whereas the resistance contribution of the domain wall occurs on the length of the domain wall width  $d_{\text{DW}}$ . Thus the relative resistance increase inside the domain wall  $(\frac{\Delta R}{R})_{\text{DW}}$  scales with  $L/d_{\text{DW}}$  [21]. Furthermore, we have to take into account that the ML is grown onto a buffer layer which acts as a parallel shunt. Thus, to determine the relative resistance increase inside the single domain wall from the experimental data  $(\frac{\Delta R}{R})_{\text{exp}}$ , we use

$$\left(\frac{\Delta R}{R}\right)_{\text{DW}} = \left(\frac{\Delta R}{R}\right)_{\text{exp}} f(\text{buffer}) \frac{L}{d_{\text{DW}}}, \quad (1)$$

where  $f(\text{buffer}) \approx 1.4$  is calculated on the basis of a shunt circuit between the magnetic material and the Pt buffer. The resistivity of the Pt buffer ( $\rho_{\text{Pt}} = 74 \mu\Omega \text{cm}$ ) is determined by measuring the resistance of single 5 nm thick Pt wires. The domain wall width has been determined by  $d_{\text{DW}} \approx \pi \sqrt{\frac{A}{K_{\text{eff}}}}$  where  $A = 5 \times 10^{-12} \text{Jm}^{-1}$  is taken from our  $M(T)$  measurements and  $K_{\text{eff}} = 1.05 \times 10^6 \text{Jm}^{-3}$ . This leads to  $d_{\text{DW}} = 7$  nm, which is a reasonable value for materials with strong out-of-plane anisotropy [22]. The DWR has been determined for four different wires, where the width of the wires has been varied between 300 and

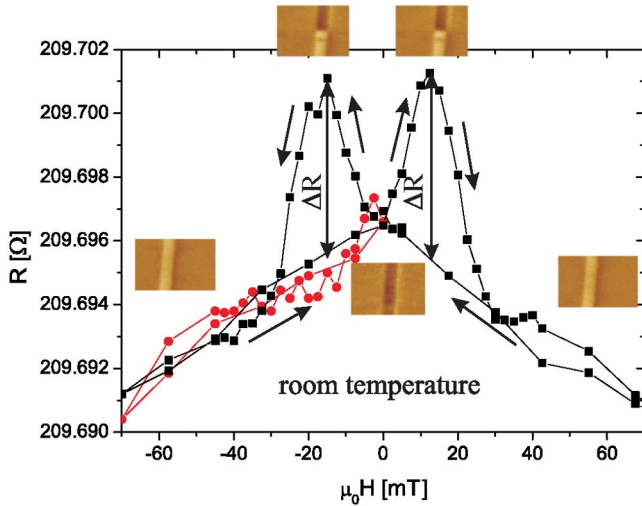


FIG. 6 (color online). Averaged MR measurement of a structure comparable to that shown in Fig. 5, however, only with one pinning center for a single domain wall. The wire has a width of  $w = 415$  nm. The red circles show the reversible behavior when the magnetic field is not reversed. When reversing the magnetic field direction (black squares) one observes resistance maxima due to the presence of a single domain wall.

450 nm. In these wires one or two domain walls are pinned as controlled by MFM. For all wires, we find for the relative resistance increase per one single domain wall a mean value of  $(\frac{\Delta R}{R})_{\text{DW}} = 1.8\%$  at room temperature where  $(\frac{\Delta R}{R})_{\text{DW}}$  varies between 1.6% and 2.0%. Please note that  $d_{\text{DW}}$  is calculated from our data and is not determined directly and an additional uncertainty arises from this value. We also calculated the additional resistivity of the domain wall  $\rho_{\text{DW}} \approx 0.6 \mu\Omega \text{ cm}$ , which is in good agreement with other experimental findings [22,23].

The fact that we find a positive DWR is in contradiction to theoretical calculations based on the idea, that electron waves are dephased inside the domain wall leading to a negative DWR [3]. Dephasing is suppressed when the domain wall is removed, which enhances the resistance, provided that WEL effects are present, which is not the case as we have recently shown for  $(\text{Co/Pt})_7$  ML nanowires [13].

To explain a positive DWR, Levy and Zhang used for their calculations the same Hamiltonian which is used to understand the giant MR [2]. For the current perpendicular wall (CPW) geometry they find that  $(\frac{\Delta R}{R})_{\text{CPW}}$  depends on the resistivities  $\rho^{(\downarrow)}$  of the spin-up(-down) channels, the exchange constant  $J$ , the Fermi velocity  $v_F$ , and the domain wall width  $d_{\text{DW}}$ . We find good agreement with the model of Levy and Zhang if we calculate  $(\frac{\Delta R}{R})_{\text{CPW}} \approx 2\%$  with  $J = 0.75$  eV,  $v_F = 1 \times 10^6$  m/s,  $d_{\text{DW}} = 7$  nm and  $\rho^{\uparrow}/\rho^{\downarrow} = 3$  which are typical parameters of multilayers with perpendicular anisotropy. Our result also is in agreement with theoretical predictions made by van Gorkom *et al.* According to their model (see Fig. 2 of Ref. [4]) our experimental value is obtained with their parameters  $\gamma = 1.1$  and  $\beta \approx 2$ .

In conclusion, we have directly determined the DWR of a single domain wall at room temperature quantitatively. The domain wall has been created and pinned locally within a  $(\text{Co/Pt})_7$  ML nanowire with perpendicular magnetic anisotropy which allows us to neglect contributions from AMR and LMR when determining the DWR. The positive value of  $(\frac{\Delta R}{R})_{\text{DW}} = (1.8 \pm 0.2)\%$  agrees well with the model of Levy and Zhang.

We thank the Deutsche Forschungsgemeinschaft for financial support through No. SFB 491.

\*Electronic address: christoph.hassel@uni-due.de

- [1] R. Taylor, A. Isin, and R. V. Coleman, Phys. Rev. **165**, 621 (1968).
- [2] P. Levy and S. Zhang, Phys. Rev. Lett. **79**, 5110 (1997).
- [3] G. Tatara and H. Fukuyama, Phys. Rev. Lett. **78**, 3773 (1997).
- [4] R. P. van Gorkom, A. Brataas, and G. E. W. Bauer, Phys. Rev. Lett. **83**, 4401 (1999).
- [5] D. Buntinx, S. Brems, A. Volodin, K. Temst, and C. Van Haesendonck, Phys. Rev. Lett. **94**, 017204 (2005).
- [6] M. Viret, Y. Samson, P. Warin, A. Marty, F. Ott, E. Sondergard, O. Klein, and C. Fermon, Phys. Rev. Lett. **85**, 3962 (2000).
- [7] U. Ruediger, J. Yu, S. Zhang, A. D. Kent, and S. S. P. Parkin, Phys. Rev. Lett. **80**, 5639 (1998).
- [8] C. H. Marrows, Adv. Phys. **54**, 585 (2005).
- [9] J. L. Olsen, *Electron Transport in Metals* (Wiley-Interscience, New York-London, 1962).
- [10] T. R. McGuire and R. I. Potter, IEEE Trans. Magn. **11**, 1018 (1975).
- [11] B. Leven, U. Nowak, and G. Dumpich, Europhys. Lett. **70**, 803 (2005).
- [12] M. Brands, O. Posth, and G. Dumpich, Superlattices Microstruct. **37**, 380 (2005).
- [13] M. Brands, A. Carl, and G. Dumpich, Ann. Phys. (N.Y.) **14**, 745 (2005).
- [14] C. Hassel, Diplom thesis, University Duisburg-Essen, 2005.
- [15] R. A. Hajjar, M. Mansuripur, and H. P. D. Shieh, J. Appl. Phys. **69**, 7067 (1991).
- [16] U. Rüdiger, J. Yu, L. Thomas, S. S. P. Parkin, and A. D. Kent, Phys. Rev. B **59**, 11 914 (1999).
- [17] R. Hyndman, P. Warin, J. Gierak, J. Ferré, J. N. Chapman, J. P. Jamet, V. Mathet, and C. Chappert, J. Appl. Phys. **90**, 3843 (2001).
- [18] T. Devolder, Phys. Rev. B **62**, 5794 (2000).
- [19] J. Fassbender, D. Ravelosona, and Y. Samson, J. Phys. D: Appl. Phys. **37**, R179 (2004).
- [20] R. A. Hajjar, T. H. Wu, and M. Mansuripur, J. Appl. Phys. **70**, 6041 (1991).
- [21] A. D. Kent, J. Yu, U. Rüdiger, S. S. P. Parkin, J. Phys. Condens. Matter **13**, R461 (2001).
- [22] R. Danneau, P. Warin, J. P. Attané, I. Petej, C. Beigné, C. Fermon, O. Klein, A. Marty, F. Ott, Y. Samson, and M. Viret, Phys. Rev. Lett. **88**, 157201 (2002).
- [23] J. F. Gregg, W. Allen, K. Ounadjela, M. Viret, M. Hehn, S. M. Thompson, and J. M. D. Coey, Phys. Rev. Lett. **77**, 1580 (1996).